



Ecological lubrication in cold forming of sintered powder metallurgical components

Prof. Dr.-Ing. Bernd-Arno Behrens¹, Dipl.-Ing. Kai Brunotte¹, M. Sc. Dieter Bohr*¹

¹Institute of Forming Technology and Machines (IFUM), Leibniz Universität Hannover, An der Universität 2, 30823 Garbsen, Germany

Abstract

In this contribution a new lubrication approach for cold bulk metal forming is presented. By exploiting the process-related porosity of pm components as a lubricant storage, the resulting pressure of a forming process forces the stored oil to leak out lubricating the process. As a result advantages like a decrease of process time because of the lubrication step omission, and an increased deformability due to compensation of lubricating film break are expected. In addition, conversion coating, which have a negative environmental impact but are commonly used in cold bulk metal forming, can be avoided. Besides that, the porosity of the pm component is reduced leading to improved mechanical properties. Experimental investigations with cylindrical aluminium pm components were carried out by compression tests in dependence of initial porosity, impregnation time and lubricant. The oil saturation of all samples could be reached after 4400 min impregnation time. The relative density has an inversely proportional effect on the absolute and the relative impregnated oil quantity. The compression tests showed an increasing maximum load with decreasing oil quantity and rising relative density. Moreover, the loads determined in the reference tests tend to be greater in comparison to the novel lubrication method.

Keywords: Powder metallurgy, cold forming, endogenous lubrication

1 Introduction

Lubrication is essential in metal forming processes. It has influence on the required forming energy, the material flow, the strain and strength distribution and the resulting workpiece surfaces [1]. Consequently, tool wear and tool life are affected [2]. Generally the following demands on lubricants are made [3]: a good and constant lubrication film, high oxidation resistance, wear and friction reduction, corrosion protection, and heat removal. Additionally, in cold bulk metal forming conversion layers or coatings are required as a lubrication carrier due to the high workpiece surface expansion [4]. The mostly used conversion compositions are based on zinc-phosphates and have a negative environmental impact [5]. Besides human health risks and hazardous waste disposal, additional process steps are needed in comparison with a tool related lubrication system [6]. In addition to the actual lubricant deposition, appropriate surface pre- and after-treatments are required, leading to high equipment and energy costs [7]. In this contribution a new lubrication technique for cold metal forming is presented which waives the usage of conversion lay-

ers and its accompanying negative impacts. For this, the process-related porosity of pm (powder metallurgy) components is exploited as a lubricant storage similar to self-lubricating bearings. Such bearings were invented in the 1920s by General Motors and are known for their low maintenance requirements and pronounced emergency running characteristics [8]. In operation, the stored oil leaks out due to elastic deformation, as a result of enhanced pressure and temperature, lubricating the process. The new lubrication approach exploits this effect in cold metal forming or rather in cold sinter-forging by means of endogenous workpiece lubrication without using any conversion coatings.

The advantages of pm processes are well known. Besides high material utilisation and productivity, pm provides the possibility to create near-net shape components with high reproducibility [9]. The most common process route consists of powder mixing, shaping by double-sided pressing, and sintering. Then, in order to enhance the material properties a subsequent cold or warm sinter-forging process can be included. In

this regard, several investigations were carried out focusing on different aspects. In consideration of the presented topic, in the following some studies, employing cold sinter-forging, are pointed out. In [10] the deformation behaviour of iron-based pm cylinders in dependence of different aspect ratios, initial porosities and standard lubrication conditions were investigated. Narayanasamy et al. studied the densification of aluminium cylinders containing low fractions of iron as a function of particle size by means of compression tests [11]. In [12] sintered Fe-C-Mn components were subjected to upsetting experiments, varying the aspect ratio and the strain. Prasanna Kumar et al. focused their studies on the density enhancement of Fe-Al₂O₃ mmc (metal matrix composite) components by closed die sinter-forging [13]. As a result, all studies show a pronounced density increase with a rising strain, leading to enhanced mechanical properties.

2 Experimental

2.1 Materials

For the experimental investigations an aluminium powder was mixed with 0.5 wt.-% wax and 0.5 wt.-% magnesium in order to increase both, the green and sintered strength [14]. The particle size and chemical composition are depicted in Table 1.

For the impregnation and compression tests two different oils were used, namely MF155 (Bechem) which is usually employed in cold bulk metal forming, and Turmofluid HPL (Lubcon), a common self-lubricating bearing oil. The major difference is the viscosity, which is ~120 mm²/s for MF155 and ~50 mm²/s for Turmofluid HPL (at 40 °C). The viscosity influence is studied in order to investigate impregnation and leak-out behaviour during compression

2.2 Sample fabrication and impregnation

Cylindrical porous aluminium samples were compacted with a double-sided tool on a hydraulic press (multi-axis powder press, SMS Meer) and were subsequently sintered in a vacuum furnace (HTK 8, Gero). The employed time-temperature-course is depicted in Figure 1. In order to burn off the wax a debinding stage at 360 °C was integrated, which is followed by the actual sintering stage at 580 °C for 40 min. After cooling down to 200 °C furnace temperature, the samples were taken out and cooled at normal air atmosphere.

The dimensions of the sintered products were constant with a diameter $d = 30 \pm 0.02$ mm and a height $h = 30 \pm 0.21$ mm. After sintering the relative density was determined by weight and volume measurements with

respect to equation (1).

$$\rho_{\text{rel}} = \frac{m/V}{\rho_{\text{theo}}} \quad (1)$$

ρ_{rel} : relative density (green or sintered)

m : weight of sintered or green part

V : volume of sintered or green part

The theoretically achievable pore-free density of the powder mix was calculated with equation (2).

$$\rho_{\text{theo}} = 100 / \sum_i \frac{w_i}{\rho_i} \quad (2)$$

ρ_{theo} : theoretical pore-free density

w_i : weight percentages of element i

ρ_i : density of element i

It was varied in two steps, approximately 0.8 and 0.9, by adjusting the pressing parameters. For the oil impregnation the samples were dived into a container with the respective oil, being completely covered.

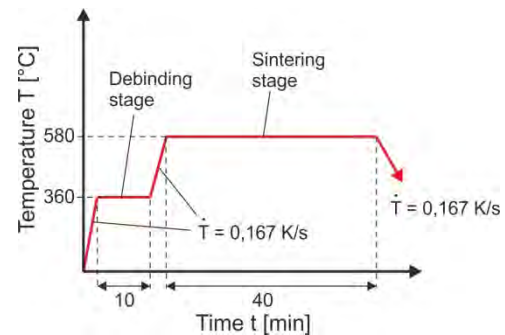


Fig. 1: Time-temperature-course for sintering of aluminium samples

The impregnation time was varied in three steps, 60 min, 180 min and 4400 min (or rather 3 days). After impregnation the entered oil quantity was determined by measuring the weight gain on a precision scale.

2.3 Compression tests

The sintered and impregnated parts were cold upset on a double-acting hydraulic press (Schirmer+Plate, type SOP II) with a maximum pressing force of 12,250 kN. This method allows characterising the workability of cold bulk sinter-forging processes [15, 16]. The tool concept is depicted in Figure 2. The dies were made of wear resistant tool steel X40CrMoV511 and the active surfaces were ground to a roughness of $R_z = 1.6$ μm .

The samples were compressed to a strain of $\phi = 0.7$, which corresponds a height reduction of approximately 15 mm or rather 50 %. The punch speed was constant

Tab. 1: Chemical composition and particle size distribution of the used powder

Chemical composition											
Element	Al	Fe	Si	Cu	Mn	Mg	Cr	Zn	Ti	Pb	Sn
Wt.-%	> 99	0.15	0.1	0.05	0.01	0.5	0.005	0.01	0.045	0.01	0.01
Particle size distribution											
Particle size	> 100 μm			> 63 μm			> 45 μm			< 45 μm	
Wt.-%	0,0			43,0			44,4			12,6	

with $v = 1$ mm/s. During upsetting the punch force and displacement were recorded using a load cell and a mechanical transducer. Except for the reference tests, no extra lubrication was used.

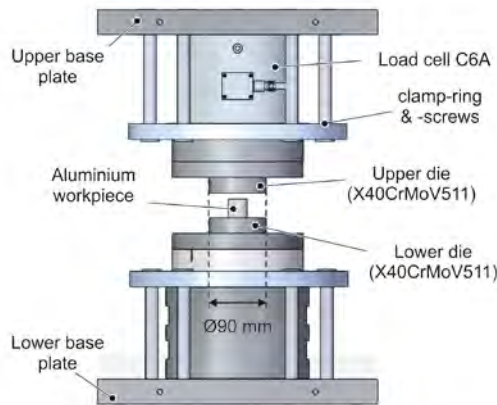


Fig. 2: Schematic tool concept for compression tests

The experimental design is summarised in Table 2. It was conducted full-factorial with 5 repetitions for each parameter combination in order to provide an adequate statistical basis for the results.

Tab. 2: Parameter variation for sample manufacturing

Relative sintered density [-]	Impregnation time [min]	Oil viscosity [mm ² /s]
0.8; 0.9	0; 60; 180; 4400	50 (HPL); 120 (MF155)

3 Results

3.1 Pressing and sintering

In Figure 3 (left) the relative sintered density of all investigated samples as a function of the respective relative green density is depicted. An additional diagonal separation line is plotted, which represents the border of density increase or decrease after sintering. Moreover, the above described target densities of $\rho = 0.8$ and $\rho = 0.9$ are highlighted. On the right-hand side of Figure 3 micrographs of the two target densities are shown, which exemplify the residual porosities.

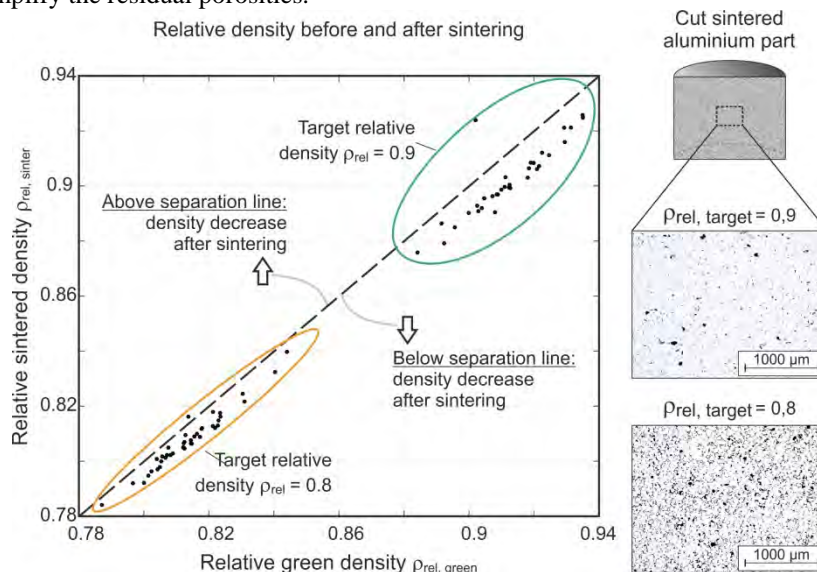


Fig. 3: Relative sintered density of all samples as a function of the green density (left) and micrographs of two samples (right)

As expected, and as already known from relevant literature, the relative density of suchlike aluminium powder compositions tends to result in slightly lower values after sintering [17, 18]. After sintering the dimensions were unaffected but a weight reduction of 0.51 ± 0.07 wt.-% (standard deviations) was measured, which can be attributed to a complete burn off process of the pressing additive. Furthermore, a minor deviation from the target densities is recognisable. Although the adjusted pressing parameters were constant, the actual densities differ from the targeted with a maximum range of 0.056. This can be explained by the process and press related imprecision. Due to process related temperature increase of the press working fluid, minor expansions occur. This leads to slight geometrical deviations of the stroke and finally to differing green products. Furthermore, deviations may occur due to the process-related manual filling process.

3.2 Impregnation

In Figure 4(a) a contour plot of the entered oil quantity as a function of relative sintered density and impregnation time for all samples is depicted. The contour is derived from a respective surface fit with a coefficient of determination of $R = 0.95$ and consequently presents a good agreement with the actual experimental results. The following 2nd degree polynomial equation for the oil quantity was employed:

$$f(x,y) = c_0 + c_0*x + c_2*y + c_3*x*y + c_4*y^2 \quad (3)$$

The variables and coefficients are given by Table 3.

Tab. 3: Variables and coefficients of surface fit function for impregnated oil quantity

Coefficients	c0	c1	c2	c3	c4
	0.95	0.43	-0.49	-0.16	0.06
Variables	f	x	y		
	Oil quantity [g]	Impregnation time [min]	Relative sintered density		

In general, with increasing density the impregnated oil quantity decreases. Due to the fact that the porosity

equals the residual quantity of relative density to one, the pore volume and subsequently the space which can be filled with oil decreases with increasing density. The smallest amount of 0.14 g oil is reached at a relative density of 0.92 and an impregnation time of 60 min, while the greatest one equals 2.7 g at 4400 min impregnation time and 0.784 relative density.

In order to examine the impregnation values autonomously from the effectively provided pore volume, a specification is applied. In fact, the impregnated oil volume is referenced to the available pore space, which results in the parameter filling ratio. In this regard, Figure 4(b) presents dependencies between the varying parameters independent of the initial pore volume. In addition, the values are grouped by oil type and target density, and regression curves are included. The general curve shapes show typical saturation behaviour. Due to the presence of closed pore networks, a full impregnation is not reached. The fraction of such networks seems to decrease when densities increase because of the generally lower filling ratios. This behaviour corresponds to the results of [19], who observed an ascending fraction of closed pores with increasing compaction pressure. In conclusion, the impregnated oil amount descends absolutely and relatively with ascending relative density.

Despite having different viscosities, the oil type has no significant influence on the impregnation behaviour. According to the Hagen-Poiseuille equation higher viscosities should lead to more pronounced capillary effects and consequently to greater filling ratios [20]. Nonetheless, such impacts are unrecognisable in this investigation as the filling ratios for the two oil types are approximately identical.

3.3 Compression tests

In Figure 5 a load-displacement diagram of two different samples and the corresponding parts after compression are depicted. A dry and an impregnated process are exemplarily confronted. The maximum load in the dry process is approximately 20 % greater compared with the lubricated one. In addition, the shell surface is more cracked in the unlubricated process. Nevertheless, cracks should be generally avoided which could be possible in a closed-die sinter-forging process.

For sound visual comparison of all samples, in the

following the maximum load F_{\max} is employed as an evaluation parameter.

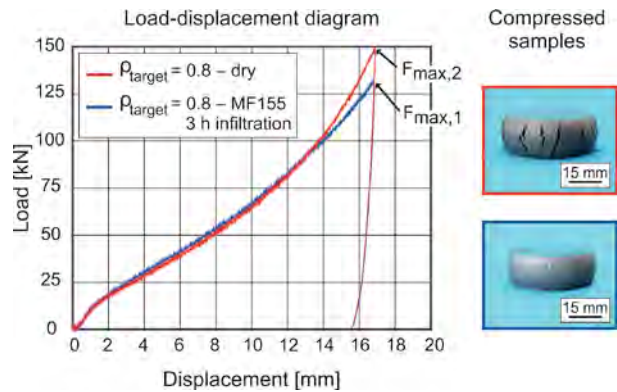


Fig. 5: Load-displacement diagram for impregnated and dry samples and the respective parts after compression

In this regard, Figure 6 (left) shows F_{\max} as a function of the impregnated oil quantity, grouped by target densities and corresponding lubrication parameters. On the right-hand side of the diagram, results of reference tests by means of conventional die lubrication and dry conditions are shown. In general, F_{\max} increases with greater densities independent of impregnated oil quantity, which corresponds with the relevant literature [11, 21, 22]. As a result of greater pore volumes which are initially closed during compression, the deformation resistance is significantly lower at smaller relative densities leading to lower maximum loads.

Furthermore, the maximum loads of the dryly and conventionally processed samples are by trend greater compared to the impregnated ones. In addition, while the reference results at higher densities seem to be similar, a difference between dry and conventional processing at lower densities is evident. Regarding the impregnated parts, two major observations can be recorded. First, the maximum load decreases with increasing oil quantity, and second, the required load is by trend lower when MF155 is employed in comparison to HPL. The first dependency can be attributed to an increasing separation effect when more lubricant is used. The second can be explained by the oil type or rather its application purpose. In contrast to HPL, MF155 is particularly designed for cold bulk metal forming and thus tends to result in decreased maximum loads.

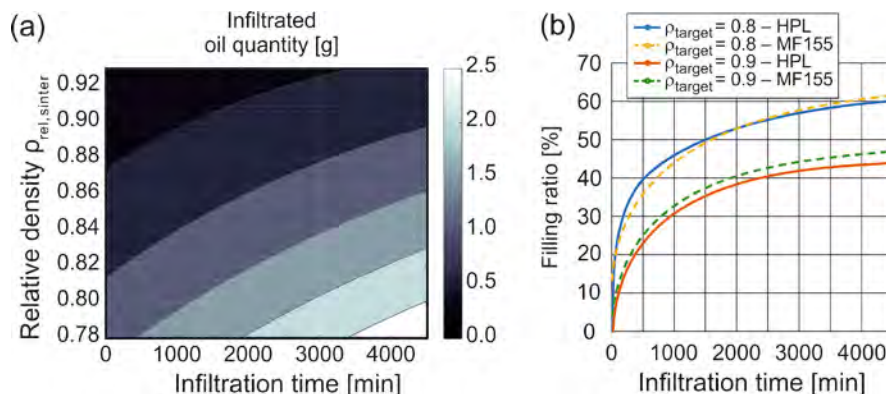


Fig. 4: Impregnated oil quantity as a function of time and relative density (a) and filling ratio as a function of time, grouped by target density and employed oil (b)

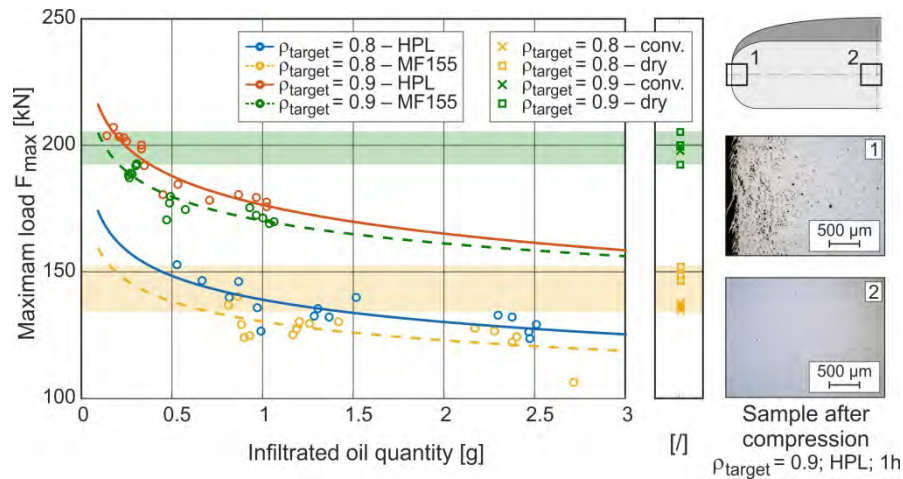


Fig. 6: Maximum load F_{max} as a function of the impregnated oil quantity, grouped by target densities and corresponding lubrication parameters (left), micrographs of compressed sample (right)

However, HPL was utilised in this contribution in order to influence and investigate the impregnation behaviour.

The compression resulted in a pronounced density increase, which can be seen on the right-hand side of Figure 6. The middle of the sample is nearly fully dense due to the major strain in this area. The bulging area has still residual porosity, which can be described with the stress distribution. In the outer surface shell process-related tensile stresses occur, which inhibit the pores to be closed. In addition, these stresses are intensified by high hydrostatic pressures within the pores, which result from the impregnated oil and increase with rising oil quantity. Thus, the oil leaks out breaking the surface partially.

4 Conclusions

In this work, a new lubrication approach for cold bulk metal forming was presented. By infiltrating porous pm components with oil, the process-related porosity was exploited as a lubricant storage. During the subsequent forming process the resulting pressure forces the stored oil to leak out lubricating the process and excluding the need to use conversion coatings. Thus, negative environmental impacts can be reduced and additional process steps, like surface pre- and after-treatments are avoided.

The described method was tested on cylindrical pm aluminium components with two different porosities ($\rho = 0.8$ and $\rho = 0.9$). Impregnation studies were carried out by varying the impregnation time ($t = [60, 120, 4400]$ min) and utilising two oil types. Subsequently, the deformation behaviour by means of compression tests was investigated.

The oil saturation of all samples could be reached after 4400 min impregnation time. The relative density has an inversely proportional effect on the absolute and the relative impregnated oil quantity. The oil type has no significant influence on the impregnation behaviour.

In the compression tests load-displacement data were recorded and the maximum load was determined. Generally, the maximum load increases with decreasing oil quantity and increasing relative density. Moreover, the loads determined in the reference tests tend to be greater in comparison to the novel lubrication method.

Acknowledgement

The presented results are based on the research project "Substitution of conventional mold lubrication by using self-lubricating raw parts in sinter forging", Project number Be1691 184-1. The authors would like to thank the German Research Foundation (DFG) for the financial support.

References

- [1] B.-A. Behrens, A. Bouguecha, T. Hadifi, J. Mielke: Advanced friction modeling for bulk metal forming processes. *Prod. Eng. Res. Devel.* 5 (2011) 621–627.
- [2] H. Paschke, M. Weber, G. Brauer, T. Yilkiran, B.-A. Behrens, H. Brand: Optimized plasma nitriding processes for efficient wear reduction of forging dies. *Archives of Civil and Mechanical Engineering* 12 (2012) 407–412.
- [3] W. J. Bartz: Selbstschmierende und wartungsfreie Gleitlager. Typen, Eigenschaften, Einsatzgrenzen und Anwendungen. *Kontakt & Studium Tribologie. expert-Verlag, Ehningen bei Böblingen* op. (1993).
- [4] H. Hofmann and J. Spindler: Verfahren der Oberflächentechnik. Grundlagen - Vorbehandlung - Beschichtung - Oberflächenreaktionen - Prüfung ; mit 72 Tabellen, zahlreichen Beispielen sowie einer CD-ROM. *Fachbuchverl. Leipzig im Carl-Hanser-Verl., München* (2004).
- [5] N. Bay: The state of the art in cold forging lubrication. *Journal of Materials Processing Technology* 46 (1994) 19–40.
- [6] M. Gariety, G. Ngaile, T. Altan: Evaluation of new cold forging lubricants without zinc phosphate precoat. *International Journal of Machine Tools and Manufacture* 47 (2007) 673–681.
- [7] F. Medea, A. Ghiotti, S. Bruschi: Temperature Effects on Organic Lubricants in Cold Forging of AA1050 Alloy. *Procedia Manufacturing* 5 (2016) 308–318.
- [8] F. V. Lenel: Powder metallurgy. Principles and applications. *Metal Powder Industries Federation, Princeton, N.J.* (1980).
- [9] W. Schatt, K.-P. Wieters, and B. Kieback: Pulvermetallurgie. *Technologien und Werkstoffe. VDI-Buch. Springer, Berlin* (2007).
- [10] C.-C. Huang, J.-H. Cheng: An investigation into the forming limits of sintered porous materials under different operational conditions. *Journal of Materials Processing Technology* 148 (2004) 382–393.
- [11] R. Narayanasamy, T. Ramesh, K. S. Pandey: Some aspects on cold forging of aluminium-iron powder metallurgy composite under triaxial stress state condition. *Materials & Design* 29 (2008) 891–903.
- [12] A. P. Mohan Raj, N. Selvakumar: Deformation Behavior of Sintered Fe-C-Mn Composite During Cold Upset Forming. *Materials and Manufacturing Processes* 26 (2011) 1388–1392.
- [13] U. J. Prasanna Kumar, P. Gupta, A. K. Jha, D. Kumar: Closed Die Deformation Behavior of Cylindrical Iron-Alumina Metal Matrix Composites During Cold Sinter Forging. *J. Inst. Eng. India Ser. D* 97 (2016) 135–151.

- [14] R. N. Lumley, T. B. Sercombe, G. M. Schaffer: Surface oxide and the role of magnesium during the sintering of aluminum. *Metall and Mat Trans A* 30 (1999) 457–463.
- [15] M. Abdel-Rahman, M. N. El-Sheikh: Workability in forging of powder metallurgy compacts. *Journal of Materials Processing Technology* 54 (1995) 97–102.
- [16] S. Narayan, A. Rajeshkannan: Workability Behaviour of Powder Metallurgy Aluminium Composites. *Journal of Powder Technology* 2014 (2014) 1–7.
- [17] A. Gökçe, F. Fındık: Mechanical and physical properties of sintered aluminum powders. *Journal of achievements in materials and manufacturing engineering* 30 (2008) 157–164.
- [18] M. Youseffi, N. Showaiter: PM processing of elemental and prealloyed 6061 aluminium alloy with and without common lubricants and sintering aids. *Powder Metallurgy* 49 (2013) 240–252.
- [19] F. J. Esper: *Pulvermetallurgie. Das flexible und fortschrittliche Verfahren für wirtschaftliche und zuverlässige Bauteile ; mit 15 Tabellen. Kontakt & Studium Bd. 494. Expert-Verl., Renningen-Malmsheim* (1996).
- [20] H. Bruus: *Theoretical microfluidics. Oxford master series in physics 18 : Condensed matter physics. Oxford Univ. Press, Oxford [u.a.]* (2011).
- [21] A. Rajeshkannan: Workability studies on cold upsetting of sintered copper alloy preforms. *Mat. Res.* 13 (2010) 457–464.
- [22] C. Sandner, R. Ratzl, B. Lorenz, T. Tobie: Sintered gears - achievable load-carrying capacities by conventional and new production methods. *International conference on Gears* (2002).